H1prelim-10-017 Submitted to

XVIII International Workshop on Deep Inelastic Scattering, DIS2010, April 19-23, 2010, Florence
Parallel Session **Small-x, diffraction and VM in DIS and hadron colliders**

Electronic Access: www-h1.desy.de/publications/H1preliminary.short_list.html

Measurement of the longitudinal diffractive structure function F_L^D at low Q^2 at HERA

H1 Collaboration

Abstract

A measurement of the longitudinal diffractive structure function F_L^D at low Q^2 using the H1 detector at HERA is presented. Measurements of the diffractive cross-section at centre of mass energies $\sqrt{s}$ of 225 and 252 GeV in the Q^2 range of $[2.5; 7]$ GeV^2, using HERA data taken in 2007, are combined with a published measurement at $\sqrt{s}$ of 300 GeV. The structure function F_L^D is extracted from these cross-sections at high values of inelasticity y. The measured values of F_L^D are compared with extrapolations of NLO QCD fits to published data, where the fits only included data with $Q^2 > 8.5$ GeV^2.

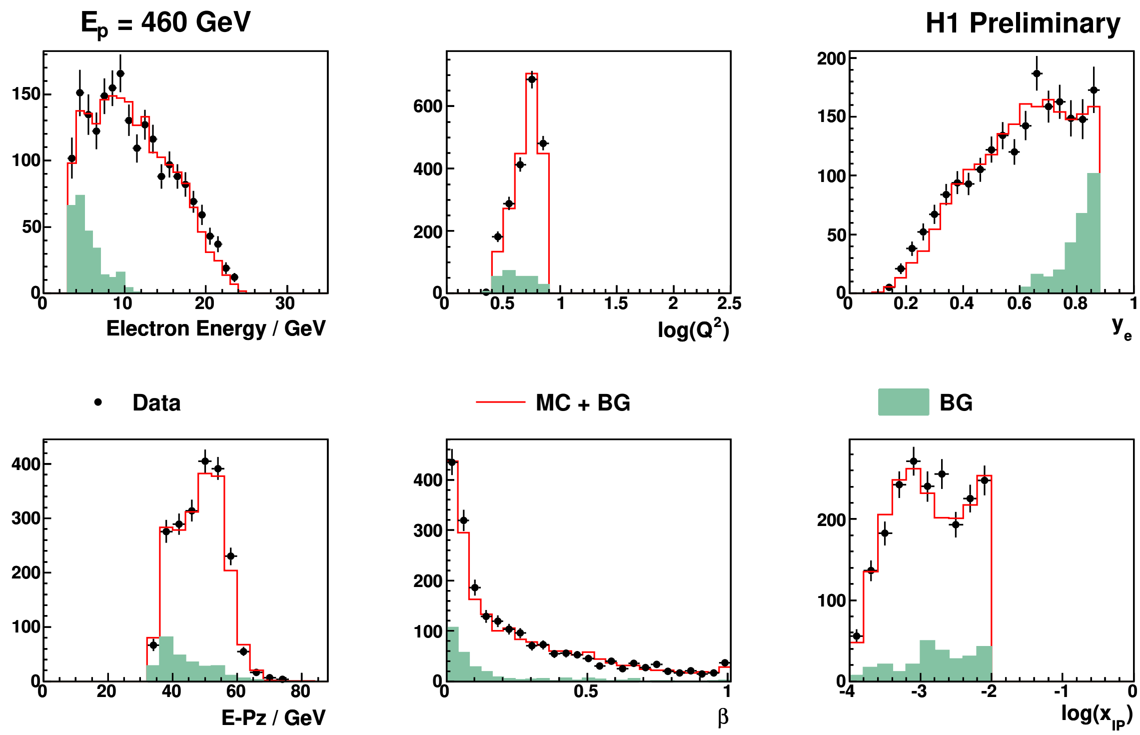

Figure 1: The electron energy, $log(Q^2)$, y_e, the summed $E - p_z$ of all final state particles, β and $x_{I\!P}$ distributions for the $E_p = 460$ GeV data. For $y_e > 0.6$, there is a requirement of positive charge of the scattered lepton candidate. Negatively charged data events (green) are used to determine the amount of photoproduction background in the region of $y_e > 0.6$. Data (points) is compared with the sum of diffractive DIS Monte Carlo (red histogram) and negatively charged events.

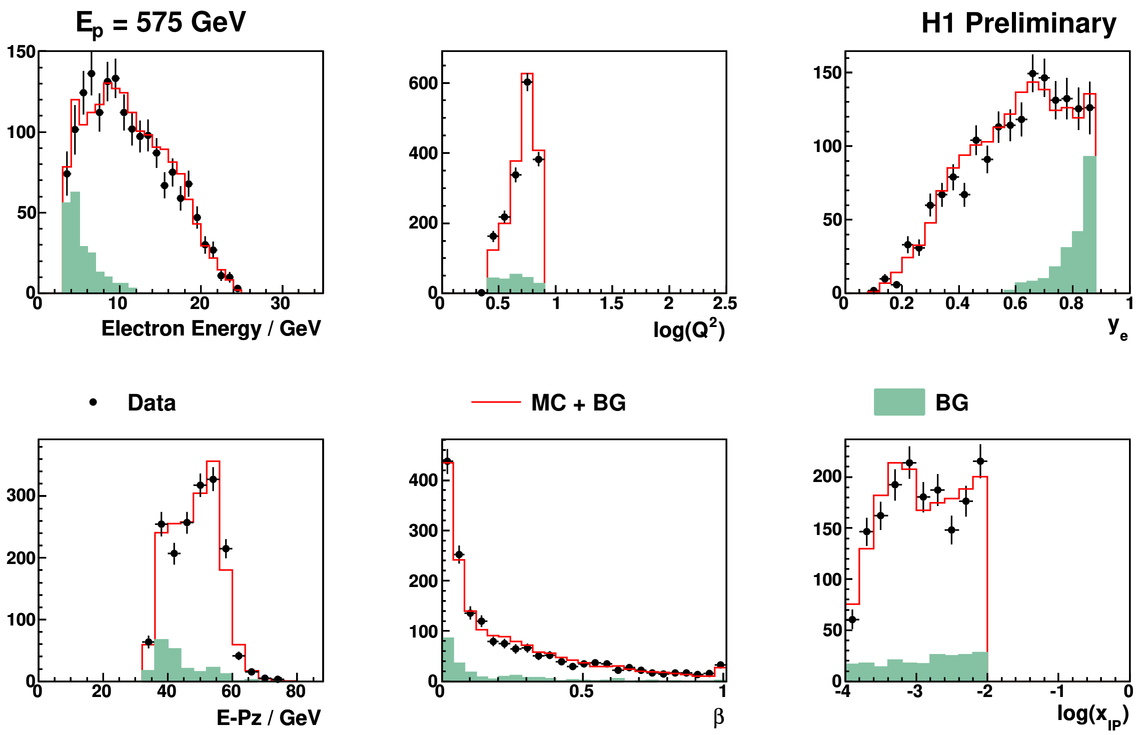

Figure 2: The electron energy, $log(Q^2)$, y_e, the summed $E - p_z$ of all final state particles, β and $x_{I\!P}$ distributions for the $E_p = 575$ GeV data. For $y_e > 0.5$, there is a requirement of positive charge of the scattered lepton candidate. Negatively charged data events (green) are used to determine the amount of photoproduction background in the region of $y_e > 0.5$. Data (points) is compared with the sum of diffractive DIS Monte Carlo (red histogram) and negatively charged events.

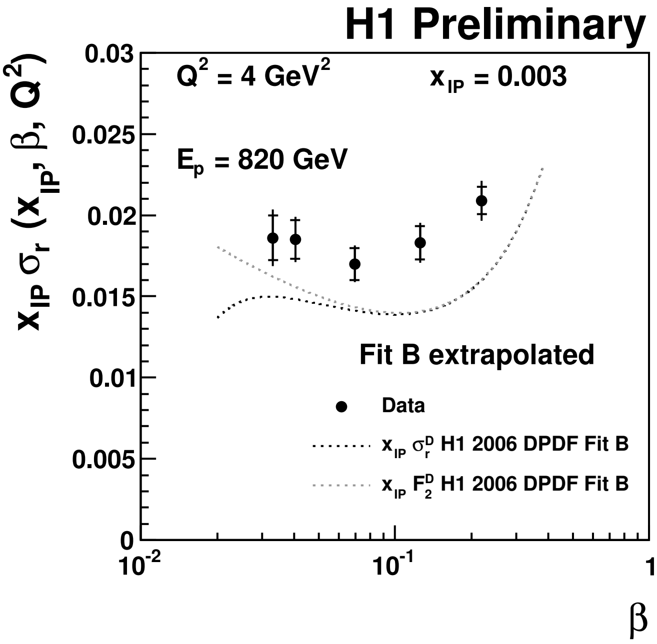

Figure 3: Previous measurement of the reduced cross-section at $E_p = 820$ GeV. The published cross-sections are recalculated at the $x_{I\!P}$, Q^2 and β values chosen for the low Q^2 F_L^D measurement. The data are compared to the H1 2006 DPDF Fit B which use the same data set starting at Q^2 of 8.5 GeV^2. The fit is extrapolated to $Q^2 = 4$ GeV^2 where it is known to underestimate the diffractive cross-section. Also shown is the prediction for F_2^D from the same fit. The inner error bars are statistical, outer error bars show the statistical and systematic errors added in quadrature.

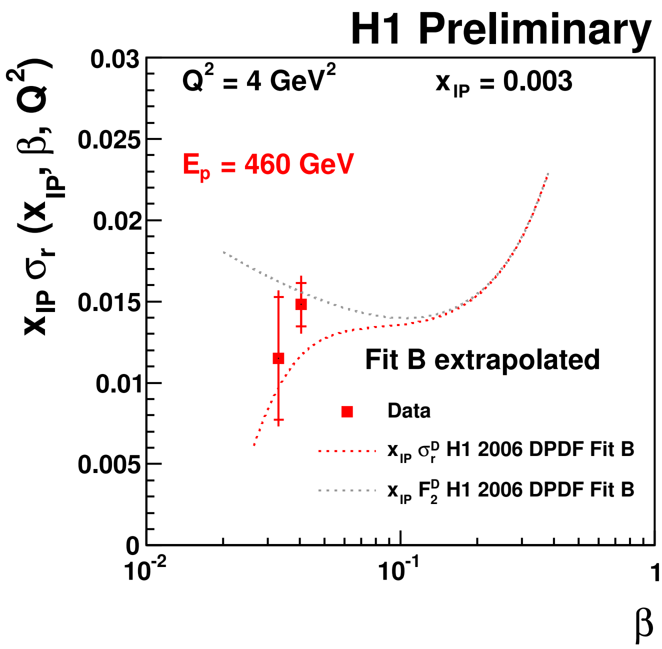

Figure 4: Measurement of the reduced cross-section at $E_p = 460\ \mathrm{GeV}$. The data are compared to a low Q^2 extrapolation of an NLO QCD fit to previous H1 data, H1 2006 DPDF Fit B, which use data starting at Q^2 of 8.5 GeV^2. The fit is extrapolated to $Q^2 = 4\ \mathrm{GeV}^2$ where it is known to underestimate the diffractive cross-section. Also shown is the prediction for F_2^D from the same fit. The inner error bars are statistical, outer error bars show the statistical and systematic errors added in quadrature.

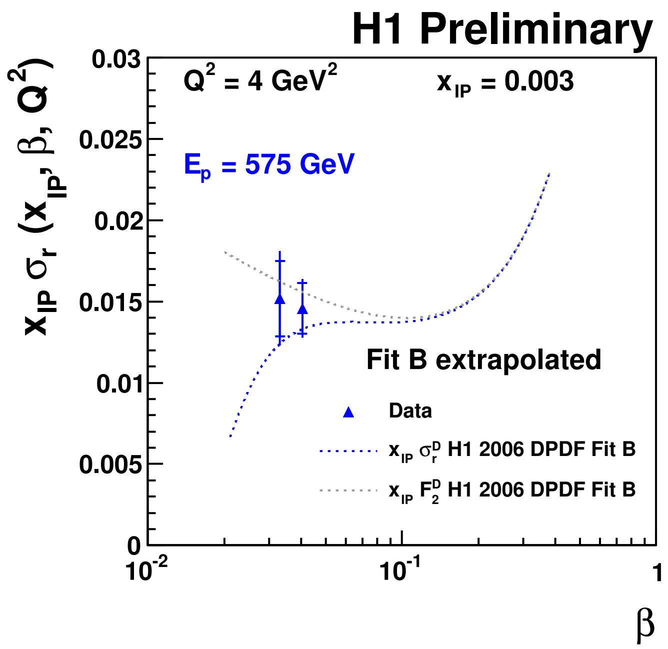

Figure 5: Measurement of the reduced cross-section at $E_p = 575$ GeV. The data are compared to a low Q^2 extrapolation of an NLO QCD fit to previous H1 data, H1 2006 DPDF Fit B, which use data starting at Q^2 of 8.5 GeV^2. The fit is extrapolated to $Q^2 = 4$ GeV^2 where it is known to underestimate the diffractive cross-section. Also shown is the prediction for F_2^D from the same fit. The inner error bars are statistical, outer error bars show the statistical and systematic errors added in quadrature.

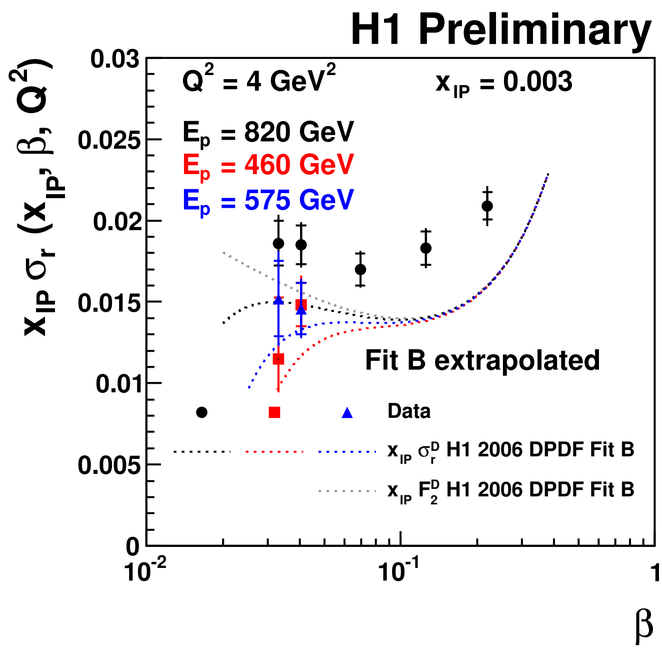

Figure 6: New measurement of the reduced cross-section at $E_p = 460, 575$ GeV, together with the combination of previously published cross sections at $E_p = 820$ GeV. The data are compared to a low Q^2 extrapolation of an NLO QCD fit to the H1 data at $E_p = 820$ GeV, H1 2006 DPDF Fit B, which use data starting at Q^2 of 8.5 GeV^2. The fit is extrapolated to $Q^2 = 4$ GeV^2 where it is known to underestimate the diffractive cross-section. Also shown is the prediction for F_2^D from the same fit. The inner error bars are statistical, outer error bars show the statistical and systematic errors added in quadrature.

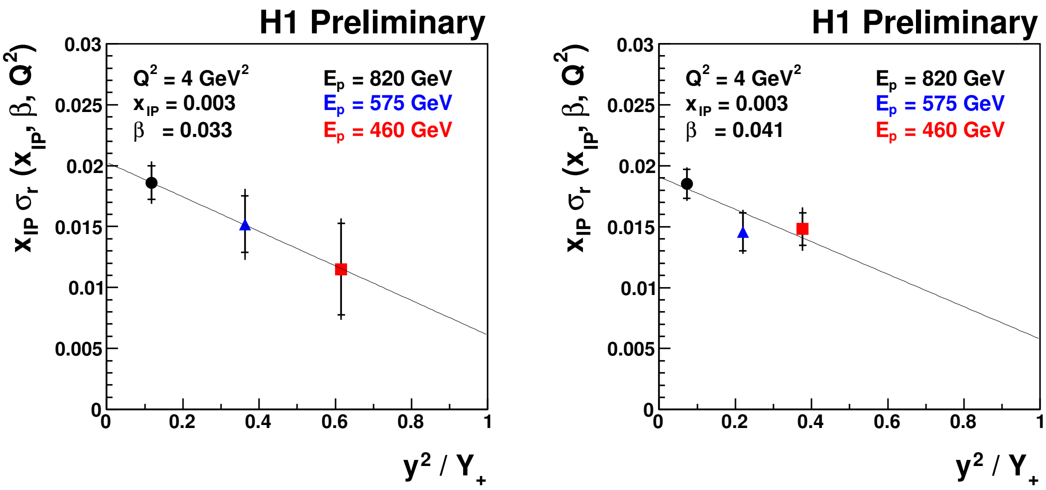

Figure 7: The reduced cross-section measured at $Q^2 = 4\ GeV^2$ and different bins of β as a function of $y^2/[(1+(1-y)^2)]$ for $E_p = 460$ (red squares), $E_p = 575$ (blue triangles) and $E_p = 820$ (black circles) GeV are shown. The inner error bars are statistical, outer error bars show the statistical and systematic errors added in quadrature. The straight lines show the linear fits use to determine F_L^D.

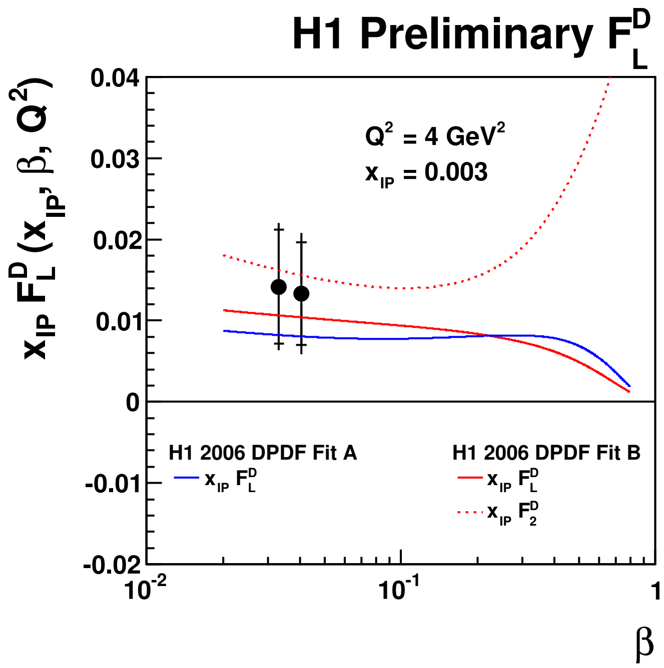

Figure 8: The diffractive longitudinal structure function F_L^D multiplied by $x_{\mathbb{P}}$, measured in the Q^2 range of $[2.5; 7]$ GeV^2 and $x_{\mathbb{P}}$ of $[0.001; 0.01]$. The data are compared to predictions from two NLO QCD fits to previous H1 data, H1 2006 DPDF Fit A (blue line) and Fit B (red line). Also shown is the value of F_2^D as a dotted red line. The fits use data starting at Q^2 of 8.5 GeV^2. Here, they are extrapolated to $Q^2 = 4$ GeV^2 where they are known to underestimate the diffractive cross-section. The data are consistent with the extrapolated fit.

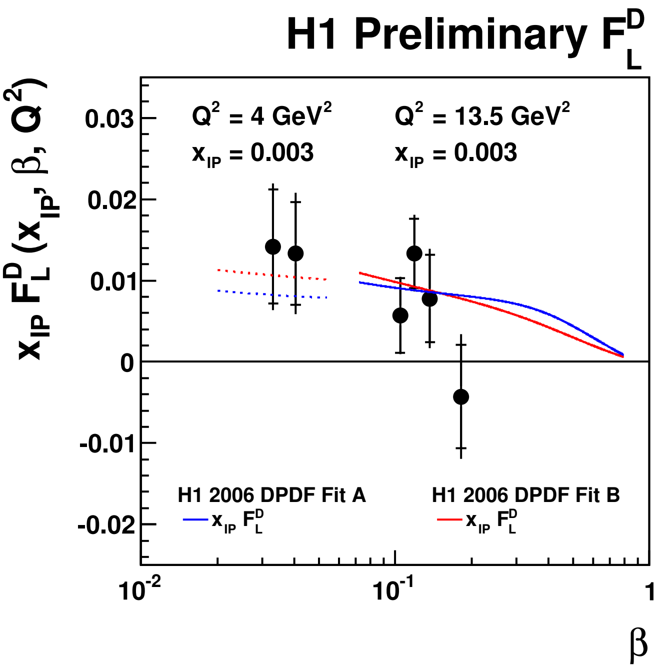

Figure 9: The diffractive longitudinal structure function F_L^D multiplied by $x_{I\!P}$. The new measurement at $Q^2 = 4$ GeV^2 is shown together with the first measurement of F_L^D, performed by the H1 Collaboration at $Q^2 = 13.5$ GeV^2. The data are compared to predictions from two NLO QCD fits to previous H1 data, H1 2006 DPDF Fit A (blue line) and Fit B (red line). The fits use data starting at Q^2 of 8.5 GeV^2. They are extrapolated to $Q^2 = 4$ GeV^2 (dotted lines) where they are known to underestimate the diffractive cross-section. The data are consistent with both predictions at $Q^2 = 13.5$ GeV^2, and their extrapolations to $Q^2 = 4$ GeV^2.